RF Transmitter Architectures and Circuits

Behzad Razavi
Electrical Engineering Department
University of California, Los Angeles

Abstract

This paper describes the design of RF transmitters for wireless applications. Following a review of constant- and variable-envelope modulation, general issues regarding the baseband/RF interface and the power amplifier/antenna interface are introduced. Various transmitter architectures are then presented and the design of upconversion mixers and power amplifiers is studied. Examples of state of the art are also described.

I. Introduction

The design of RF transmitters for wireless applications entails many challenges at both architecture and circuit levels. The number of off-chip components, the restrictions on unwanted emissions, and the trade-offs between the output power, the efficiency, and the required linearity directly impact the choice of the transmitter topology and the implementation of each circuit block. Furthermore, the disturbance of the transceiver's oscillators and receive path by the transmit path influences the frequency planning and limits the level of integration.

This paper provides an overview of RF transmitter design for wireless systems with emphasis on high levels of integration. Focusing on mobile units, the paper begins with a review of constant- and variable-envelope modulation and a study of general transmitter design issues in Section II. Transmitter architectures are described in Section III and the design of building blocks in Section IV. Examples of the state of the art are presented in Section V.

II. General Considerations

An RF transmitter performs modulation, upconversion, and power amplification, with the first two functions combined in some cases. Transmitter design requires a solid understanding of modulation schemes because of their influence on the choice of such building blocks as upconversion mixers, oscillators, and power amplifiers (PAs). In this section, we briefly describe two commonly-used modulation formats and their design implications.

A. Constant- and Variable-Envelope Modulation

Modulation formats generally exhibit trade-offs between bandwidth efficiency, power efficiency, and detectability. In today's mobile communications, all three parameters are important because they determine the capacity, the talk time, and the maximum range, respectively. The design of transmitters deals with primarily the trade-off between bandwidth efficiency and power efficiency, an issue arising from the properties of "constant-envelope" (or "nonlinear") and "variable-envelope" (or "linear") modulation schemes.

A modulated signal $x(t) = A\cos[\omega_c t + \phi(t)]$ has a constant envelope if A does not vary with time. Such a waveform carries information in only the zero-crossing points and can therefore be processed by a nonlinear power amplifier with high power efficiency. A simple example, used in paging applications, is binary frequency shift keying (BFSK), whereby the baseband rectangular pulses are directly applied to a voltage-controlled oscillator (VCO) [Fig. 1(a)]. In this case, $\phi(t) = K_{VCO}\int x_{BB}(t)dt$, where K_{VCO} is the gain of

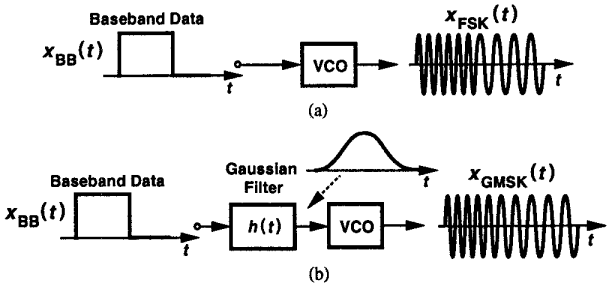

Fig. 1. Generation of (a) FSK and (b) GMSK signals.

the VCO and $x_{BB}(t)$ the baseband signal.

While exhibiting a constant envelope, BFSK signals occupy a relatively wide spectrum, partly owing to the abrupt frequency jumps introduced by the sharp edges of the baseband pulses. If the frequency changes more smoothly from one bit to the next, then the required bandwidth decreases. To this end, Gaussian minimum shift keying (GMSK) alters the shape of the baseband pulses so as to vary the frequency gradually. As shown in Fig. 1(b), the rectangular pulses are first applied to a Gaussian filter, thereby generating smooth edges at the input of the frequency modulator. The resulting output is expressed as

$$x_{GMSK}(t) = A\cos[\omega_c t + K_{VCO}\int x_{BB}(t) * h(t)dt], \quad (1)$$

where $h(t)$ is the impulse response of the Gaussian filter.

Used in standards such as GSM, DECT, HIPERLAN, and

0-7803-5443-5/99/$10.00©1999 IEEE

the frequency-hopped version of IEEE 802.11, GMSK modulation lends itself to nonlinear amplification while consuming a moderate bandwidth. Note, however, that the Gaussian shaped pulses in Fig. 1(b) suffer from overlap in the time domain, introducing intersymbol interference.

The conceptual modulation method of Fig. 1(b) is indeed employed in some transmitters, e.g., in DECT. However, if the amplitude of the baseband signal applied to the VCO or the gain of the VCO are poorly controlled, so is the bandwidth of the modulated signal. For this reason, in high-precision systems such as GSM, the waveform in (1) is rewritten as $x_{GMSK}(t) = A\cos\omega_c t\cos\theta - \sin\omega_c t\sin\theta$, where $\theta = K_{VCO}\int x_{BB}(t) * h(t)dt$, and $\cos\theta$ and $\sin\theta$ are generated by accurate mixed-signal techniques [1, 2].

Variable-envelope signals are also used in many communication systems. Such signals can be expressed as $x(t) = A(t)\cos[\omega_c t + \phi(t)]$, where $A(t)$ is the envelope. The variation of $A(t)$ with time is undesirable but typically inevitable in linear modulation schemes designed to occupy a small bandwidth. Consider a quadrature phase shift keying (QPSK) waveform with abrupt phase jumps [Fig. 2(a)]. Expressed as $x(t) = a(t)\cos\omega_c t + b(t)\sin\omega_c t$, where $a(t)$ and $b(t)$ are sequences of binary rectangular pulses, the signal can be generated as shown in Fig. 2(b), indicating the output spectrum is of the form $[\sin(\pi T_S f)^2]/(\pi T_S f)^2$, where T_S denotes the width of one pulse. Such a waveform *can* be amplified nonlinearly without corruption of the information, but it consumes substantial bandwidth.

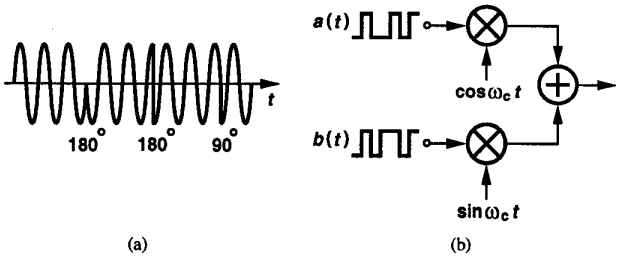

Fig. 2. (a) QPSK waveform, (b) generation of QPSK signal from baseband streams.

In order to tighten the spectrum of QPSK waveforms, the baseband pulses are altered from a rectangular form to a shape exhibiting a more compact spectrum. A popular format is "raised-cosine" filtering, where each bit is represented by a sinc-like waveform (Fig. 3). The actual expressions for the time-domain and frequency-domain representations of raised-cosine signals can be found in [2], but we point out that the resulting spectrum approaches a "box" shape, providing high bandwidth efficiency.

Used in standards such as IS-54, IS-95, and the direct-sequence spread-spectrum version of IEEE 802.11, QPSK modulation with raised-cosine filtering[1] occupies minimal bandwidth but suffers from a variable envelope.[2] As illustrated in Fig. 4, at every phase transition point the waveform experiences a "ripple" in the envelope whose magnitude is proportional to the change in phase. If such a signal is applied to a nonlinear PA, then the output exhibits significant power in adjacent channels (Fig. 5) (an effect called "spectral regrowth") [2], possibly violating emission mask requirements of the standard. For this reason, the above standards incorporate linear - inevitably inefficient - power amplifiers while conferring a high capacity.

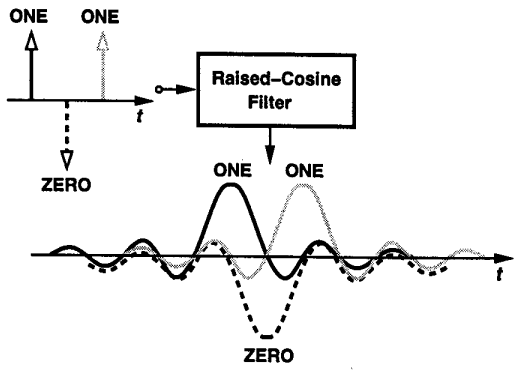

Fig. 3. Shaping baseband pulses to obtain a compact spectrum.

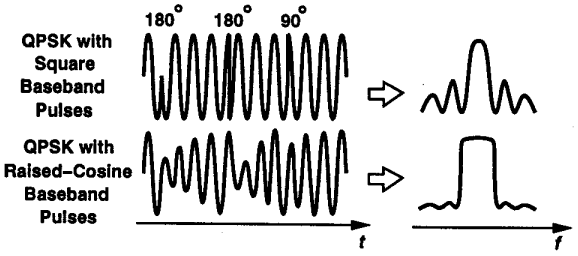

Fig. 4. Variation of envelope with raised-cosine baseband pulses.

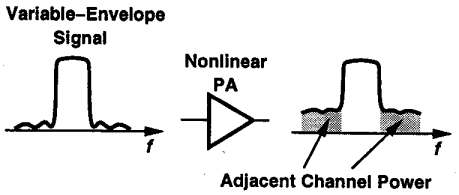

Fig. 5. Generation of adjacent power in a nonlinear PA.

B. Baseband/RF Interface

The baseband/RF interface in a transmitter performs the desired modulation and upconversion. Since square baseband pulses are generally ill-suited to bandwidth-efficient communications, first the proper pulse shape is created by table-lookup or other waveform generation techniques. For example, as illustrated in Fig. 6, each baseband pulse is oversampled, mapped to the desired shape, and constructed in the analog domain by means of a digital-to-analog converter (DAC).

The baseband/RF interface typically assumes one of two forms. For nonlinear modulation, the interface can be realized as shown in Fig. 7, where a VCO converts the input shaped pulses to frequency. In order to define the output center fre-

[1] In reality, the raised-cosine filter is decomposed into two root raised-cosine filters, one placed in the transmitter and the other in the receiver [2].

[2] Offset QPSK and $\pi/4$-QPSK exhibit less ripple.

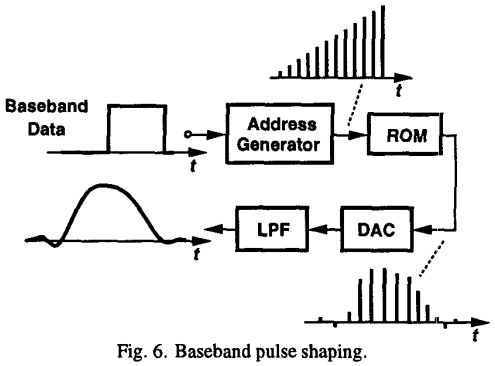

Fig. 6. Baseband pulse shaping.

Fig. 7. Baseband/RF interface in for nonlinear modulation.

quency accurately, the VCO is first placed in a synthesizer loop.

Another topology, suited to both linear and nonlinear modulation, is the quadrature upconverter depicted in Fig. 8. If $\sin\theta$ and $\cos\theta$ are generated according to our derivations in Sec-

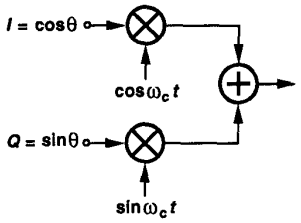

Fig. 8. Quadrature upconverter for linear and nonlinear modulation.

tion II.A, then the output is a phase- or frequency-modulated signal. For linear modulation formats such as QPSK with raised-cosine filtering, we can write

$$x_{QPSK} = \sum_n a_n p(t-nT_S)\cos\omega_c t + \sum_n b_n p(t-nT_S)\sin\omega_c t, \tag{2}$$

where $a_n, b_n = \pm 1$ and $p(t)$ denotes the desired pulse shape. Thus, as shown in Fig. 9, the single stream of rectangular pulses baseband pulses is first decomposed into two streams at half the rate and subsequently shaped and applied to the quadrature modulator.

C. PA/Antenna Interface

RF transmitters employ a carefully designed amplifier and matching network to deliver the required power to the antenna. Fig. 10 depicts a typical configuration, where a duplexer filter separates the transmit (TX) and receive (RX) bands [in the case of frequency-domain duplexing (FDD)]. If the TX and RX bands coincide, the duplexer is replaced by an RF switch to perform time-domain duplexing (TDD). The duplexer filter suffers from a loss of 2 to 3 dB, thereby dissipating 30% to 50% of the PA output in the form of heat. For TDD switches, on the other hand, the loss is in the range of 0.5 to 1 dB. While this issue makes TDD more attractive in power-conscious applica-

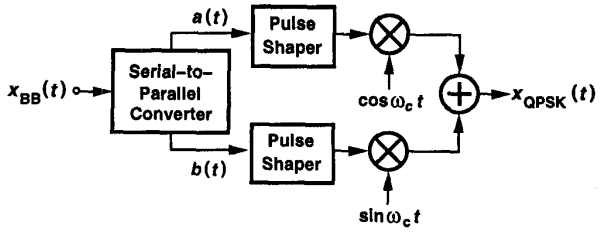

Fig. 9. QPSK modulation with pulse shaping.

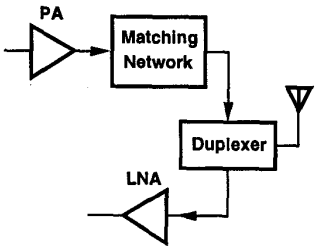

Fig. 10. PA/antenna interface.

tions, FDD is more widely used in stringent cellular systems so as to ensure that the high-power signals transmitted by the users do not fall in their own receive band.

In addition to substantial loss of power, duplexers also introduce feedthrough from the transmit band to the receive band. Illustrated in Fig. 11, this effect arises simply because of the finite attenuation of the TX filter in the receive band - only

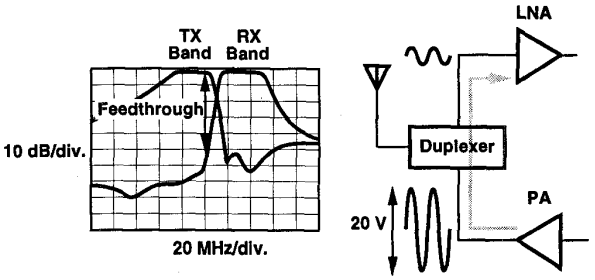

Fig. 11. Feedthrough from TX path to RX path.

45 to 50 dB at the edge. (In practice, the leakage through the duplexer package or the printed circuit board may exacerbate the issue.) The feedthrough of the PA output to the LNA input creates two difficulties. (1) The large signal generated by the PA heavily desensitizes the receiver. For example, if the PA delivers +30 dBm and the feedthrough is −50 dB, then the receiver experiences an input of −20 dBm, a level comparable with the 1-dB compression point of many receiver designs. (2) The thermal noise at the output of the PA raises the input noise floor of the receiver. For example, if the PA thermal noise is −120 dBm/Hz and the leakage in the middle of the RX band is −60 dB, then the thermal noise introduced in the receive band reaches −180 dBm, only 6 dB higher than the available thermal noise power from the antenna. This issue requires that the entire TX path be designed for low noise.

The duplexer feedthrough makes it desirable to avoid operating the TX and RX paths simultaneously. For example, in the digital mode of IS-54 and in GSM, the TX and RX

time slots are offset such that they have no overlap (Fig. 12). Note that this does not introduce any "dead" time because in a

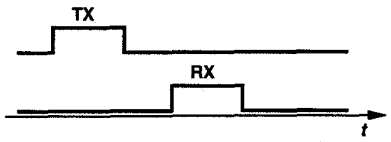

Fig. 12. Time offset between TX and RX time slots in a TDMA system.

time-division multiple access (TDMA) system, each user finds access to the network for only part of the time. Such an offset also allows sharing some of the transceiver's components, e.g., oscillators and synthesizers, between the TX and RX paths. (In principle, much of the supply current can also be time-shared between the two paths.)

Simultaneous operation of the transmitter and the receiver is nonetheless necessary in some applications. For example, in the relatively old "analog" standard Advanced Mobile Phone System (AMPS), neither of the two paths can be turned off simply because of the lack of digital storage of the signal. Also, in direct-sequence spread-spectrum communication systems such as IS-95, continuous monitor and control of the transmitted power requires that the mobile unit's RX and TX paths operate simultaneously.

The signal transmitted by the antenna must comply with various emission regulations so that it does not corrupt other users' communication. GSM, for example, enforces the mask shown in Fig. 13, constraining both the modulation index

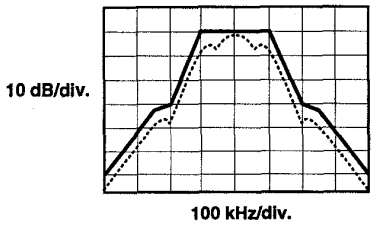

Fig. 13. GSM emission mask.

of the GMSK waveform and the design of the TX building blocks (Section IV). In standards using linear modulation, e.g., in IS-95 and the digital mode of IS-54, the adjacent-channel power ratio (ACPR) is specified. Illustrated in Fig. 14, ACPR requirements necessitate adequate linearity in the power am-

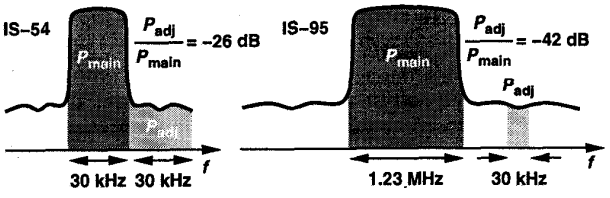

Fig. 14. ACPR in IS-54 and IS-95.

plifier and upconversion mixers. Similar regulations apply to spurs and harmonics at the output of the transmitter.

It is interesting to note that, despite the use of offset TX and RX time slots, GSM still requires a very low thermal noise emission in the receive band. This is because if two mobile users stand in proximity, then the thermal noise transmitted by one may corrupt the signal received by the other (Fig. 15).

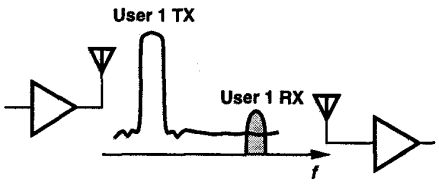

Fig. 15. Effect of TX thermal noise in RX band of another user.

III. Transmitter Architectures

The choice of a transmitter architecture is determined by two important factors: wanted and unwanted emission requirements and the number of oscillators and external filters. In general, the architecture and frequency planning of the transmitter must be selected in conjunction with those of the receiver so as to allow sharing hardware and possibly power.

A. Direct-Conversion Architecture

In direct-conversion transmitters, the output carrier frequency is equal to the LO frequency, and modulation and upconversion occur in the same circuit (Fig. 16). The simplicity of the topology makes it attractive for high levels of

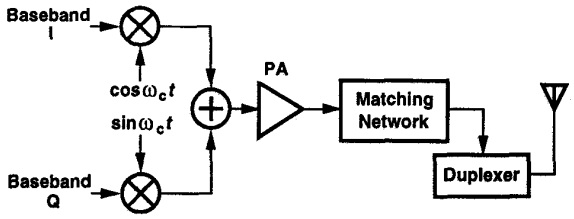

Fig. 16. Direct-conversion transmitter.

integration.

The direct-conversion architecture nonetheless suffers from an important drawback: disturbance of the local oscillator by the power amplifier output. Illustrated in Fig. 17, this issue arises because the PA output is a modulated waveform

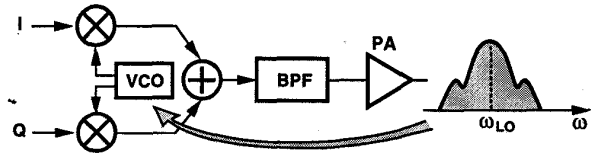

Fig. 17. LO pulling by PA.

having a high power and a spectrum centered around the LO frequency. Despite various shielding techniques employed to isolate the VCO, the "noisy" output of the PA still corrupts the oscillator spectrum. This corruption occurs through "injection pulling" or "injection locking" [3], whereby the frequency of an oscillator tends to shift towards the frequency of an external stimulus. As shown in Fig. 18, if the frequency of the injected noise is close to the oscillator natural frequency, then the LO output is disturbed increasingly as the noise magnitude rises, eventually "locking" to the noise frequency. In practice, noise

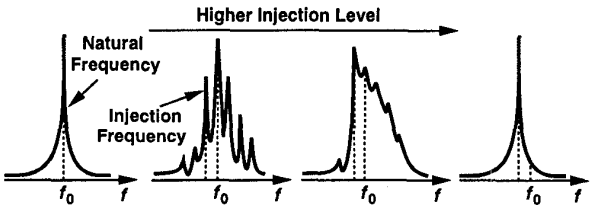

Fig. 18. Injection pulling as the magnitude of the injected noise increases.

levels as low as 40 dB below the oscillation level may create tremendous disturbance.

The phenomenon of LO pulling is alleviated if the PA output spectrum is sufficiently far from the oscillator frequency. For quadrature upconversion, this can be accomplished by "offsetting" the LO frequency, that is, by adding or subtracting the output frequency of another oscillator [4]. Fig. 19 shows an example where the output signals of VCO_1 and VCO_2 are

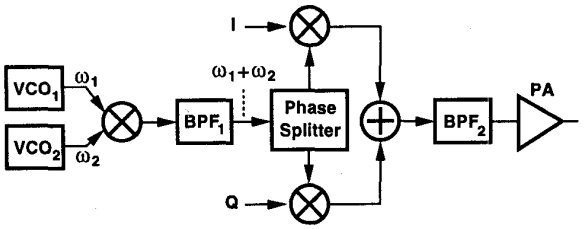

Fig. 19. Direct-conversion transmitter with offset LO.

mixed and the result is filtered such that the carrier frequency is equal to $\omega_1 + \omega_2$, far from either ω_1 or ω_2.

The selectivity of the first bandpass filter, BPF_1, in Fig. 19 impacts the quality of the transmitted signal. Owing to nonlinearities in the offset mixer, many spurs of the form $m\omega_1 \pm n\omega_2$ appear at the input of BPF_1. If not adequately suppressed by the filter, such components degrade the quadrature generation of the carrier phases as well as create spurs in the upconverted signal.

B. Two-Step Architecture

Another approach to circumventing the problem of LO pulling in transmitters is to upconvert the baseband signal in two (or more) steps so that the PA output spectrum is far from the frequency of the VCOs. As an example, consider the circuit shown in Fig. 20. Here, the baseband I and Q

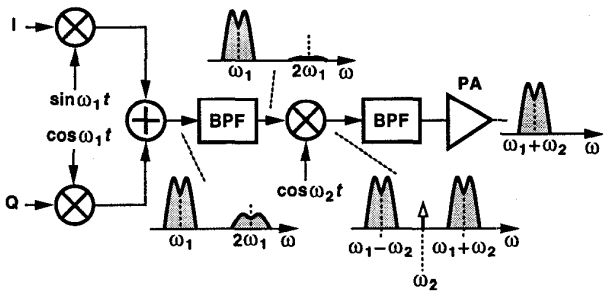

Fig. 20. Two-step transmitter.

channels undergo quadrature modulation at a lower frequency, ω_1 [called the intermediate frequency (IF)], and the result is upconverted to $\omega_1 + \omega_2$ by mixing and band-pass filtering. The first BPF suppresses the harmonics of the IF signal while the second removes the unwanted sideband centered around $\omega_1 - \omega_2$.

An advantage of two-step upconversion over the direct approach is that since quadrature modulation is performed at lower frequencies, I and Q matching is superior, leading to less cross-talk between the two bit streams (Section IV.A). Also, a channel filter may be used at the first IF to limit the transmitted noise and spurs in adjacent channels.

The difficulty in two-step transmitters is that the bandpass filter following the second upconversion must reject the the unwanted sideband by a large factor, typically 50 to 60 dB. This is because the simple upconversion mixing operation produces both the wanted and the unwanted sidebands with *equal* magnitudes. Owing to the higher center frequency, this filter is typically a passive, relatively expensive off-chip device.

C. Offset-PLL Architecture

A transmitter topology suited to systems using constant-envelope modulation is the offset-PLL architecture [5, 6]. This technique has been invented to meet the stringent GSM requirements for the thermal noise in the receive band (Fig. 15).

First, consider the circuit shown in Fig. 21, where a quadrature modulator is followed by a phase-locked loop. Here, the

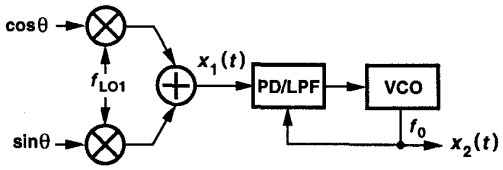

Fig. 21. Upconversion of a constant-envelope signal by means of a PLL.

PLL operates as a narrowband filter centered around f_0, suppressing the out-of-band noise generated by the modulator. If the loop bandwidth of the PLL is chosen properly, the phase information in $x_1(t)$ is transferred to $x_2(t)$ faithfully while the output noise at large frequency offsets is determined by that of the VCO. Note that the VCO phase noise exists in other architectures as well, and the advantage of the circuit of Fig. 21 is that it suppresses the noise contributed by other sources.

In practice, it is difficult to operate the phase detector of Fig. 21 at high frequencies. If a divide-by-N is inserted in the feedback path (Fig. 22), then the phase modulation of $x_1(t)$ is "amplified" by a factor of N when it appears in

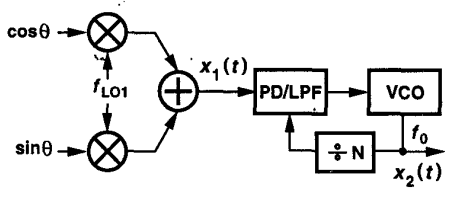

Fig. 22. Upconversion of a constant-envelope signal by means of a PLL with feedback divider.

$x_2(t)$, requiring "finer" phase modulation in $\sin\theta$ and $\cos\theta$. More importantly, since the frequency steps in f_{LO1} are also amplified by N, the synthesizer producing f_{LO1} must provide small channel spacing, suffering from a long settling time. To

alleviate these issues, as shown in Fig. 23 [5], the PLL can incorporate an offset mixer driven by another oscillator so as

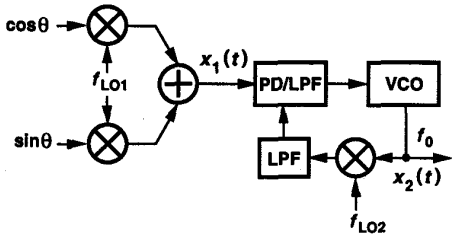

Fig. 23. Upconversion using offset PLL.

to lower the frequency presented to the PD. Note that in this case, $\sin\theta$ and $\cos\theta$ are upconverted to an IF signal such that $f_{LO2} \pm f_{LO1} = f_0$.

In the offset-PLL architecture, the quadrature upconverter can be embedded inside the loop. Shown in Fig. 24 [6], the loop senses a constant frequency, f_{REF}, thus minimizing the

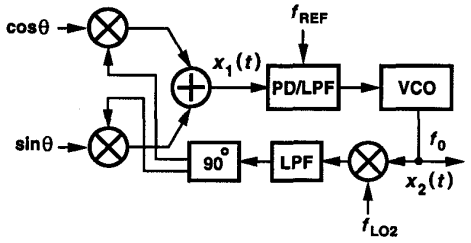

Fig. 24. Offset PLL including quadrature upconversion.

phase variation of $x_1(t)$ and hence modulating the phase of $x_2(t)$ according to the baseband waveforms.

The offset-PLL architecture requires two high-frequency VCOs and a relatively selective filter (at the output of the offset mixer), and as such is more complex than other topologies described above. Nevertheless, the low out-of-band noise offered by this configuration allows operating the transceiver *without* a duplexer, saving several tens of percent of the power delivered by the PA. With no expensive, bulky duplexers, offset-PLL transmitters are well-suited to low-cost, high-performance systems using constant-envelope modulation, but the issue of VCO pulling by the PA may be of concern here.

IV. Building Blocks

A. Upconversion Mixers

The upconversion mixers in a quadrature modulator can easily be realized as Gilbert cells, with their outputs added in the current domain (Fig. 25). Interestingly, both the linearity of the baseband ports and the phase and gain matching of the mixers impact the quality of the modulated signal. We consider the effect of nonlinearity in GMSK, e.g., the GMSK waveform of Section II.A with the assumption that $\cos\theta$ and $\sin\theta$ experience third-order distortion. The resulting signal can then be expressed as

$$\begin{aligned} x_{GMSK}(t) &= A\cos\omega_c t[\cos\theta + \alpha\cos(3\theta)] \\ &\quad -A\sin\omega_c t[\sin\theta + \alpha\sin(3\theta)], \end{aligned} \quad (3)$$

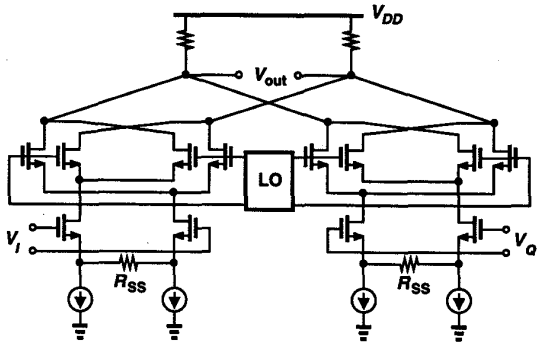

Fig. 25. I/Q upconverter using Gilbert cells.

where α represents the amount of third-order nonlinearity. Grouping the terms in (3), we obtain

$$\begin{aligned} x_{GMSK}(t) &= A\cos[\omega_c t + K_{VCO}\int x_{BB}(t) * h(t)dt] \\ &\quad +\alpha A\cos[\omega_c t + 3K_{VCO}\int x_{BB}(t) * h(t)dt]. \end{aligned} \quad (4)$$

Equation (4) reveals that third-order distortion gives rise to a component centered around ω_c but with a modulation index three times that of the ideal GMSK signal. Invoking Carson's rule [7], we note that the second term occupies roughly three times the bandwidth, raising the power transmitted in adjacent channels. Fig. 26 shows the simulated spectra of the two components in Eq. (4) with $\alpha = 1$, indicating that the unwanted signal indeed consumes a wider band. For this reason, α must be small enough that the transmission mask is not violated. Thus, the baseband port of the mixers typically incorporates resistive degeneration to achieve sufficient linearity.

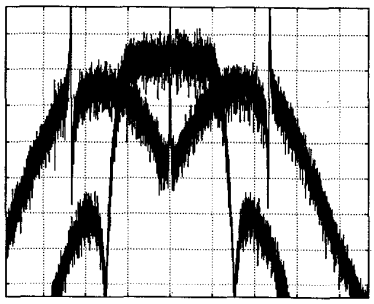

Fig. 26. Simulated spectra of the two terms in Eq. (4). (Horiz. scale normalized to bit rate, vert. scale: 5 dB/div.)

The matching of upconversion mixers is also important. Similar to the I/Q mismatch effect in direct-conversion receivers [2], this imperfection leads to cross-talk between the two data streams modulated on the quadrature phases of the carrier. A common approach to quantifying the I/Q mismatch in a transmitter is to apply two signals $V_0\sin\omega_{in}t$ and $V_0\cos\omega_{in}t$ to the I and Q input terminals and examine the spectrum produced by the adder. In the ideal case, the output in the band of interest is simply given by $V_{out}(t) = V_0\sin\omega_{in}t\sin\omega_{LO}t + V_0\cos\omega_{in}t\cos\omega_{LO}t = V_0\cos(\omega_{LO} - \omega_{in})t$. On the other hand, in the presence of a gain mismatch of ϵ and phase imbalance of θ, an unwanted sideband at

$\omega_{LO} + \omega_{in}$ appears at the output. The power of the sideband at $\omega_{LO} + \omega_{in}$ divided by that of the sideband at $\omega_{LO} - \omega_{in}$ serves as a measure of the I/Q imbalance [2]. In practice, the crosstalk between the two data streams becomes negligible if the above test yields an unwanted sideband about 30 dB below the desired signal.

B. Power Amplifiers

Power amplifiers are typically the most power-hungry building blocks of RF transceivers. The design of PAs, especially for linear, low-voltage operation, remains a difficult problem, still defying an elegant solution. In practice, PA design has involved a substantial amount of trial and error - one reason why discrete or hybrid implementations of this circuit are favored.

Suppose a PA is to deliver 1 W to a 50-Ω antenna while operating with a 3-V supply. Then, in order to generate a 20-V_{PP} swing across the antenna, the circuit must incorporate a "matching network," e.g., a transformer. Shown in Fig. 27 is a simple example indicating that the peak current in the primary

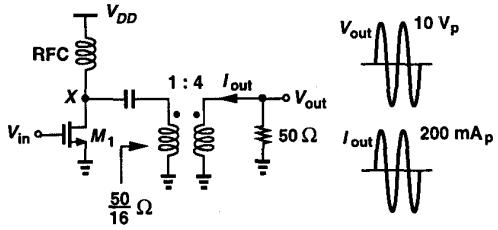

Fig. 27. Simple PA with matching network.

of the transformer exceeds 800 mA. Furthermore, M_1 must sink the currents flowing through both the radio-frequency choke (RFC) and the transformer when $V_X \approx 0$, a peak value of 1.6 A. With realistic efficiencies of 30 to 50%, the peak current through M_1 may need to be even higher.

The enormous currents in the output device and the matching network are one of the difficulties in the design of power amplifiers and especially the package. If the peak current through the output transistor is several amperes, then the slew rate at 900 MHz is on the order of 10 A/ns. Thus, even a parasitic inductance of 10 pH causes a 100-mV reduction in the voltage swing. Furthermore, parasitic inductances can introduce various resonances and even instability in the circuit. Similarly, a series resistance of a few tens of milliohms in the transistor, the RFC, or the matching network may result in a considerable loss. For these reasons, many layout and packaging issues that are usually unimportant in other analog and RF circuits become crucial in power amplifiers.

In addition to output power, efficiency, and linearity, other parameters such as the required supply voltage, spurs and harmonics, and power control are also critical in many applications. For example, in IS-95, the output power must be adjustable in 1-dB steps.

PA Classes. Among many classes of PAs, only a few have proved practical in mobile communications. The limited battery voltage and energy constrain the choice of PA topologies in portable systems.

The operation of PAs in classes A, B, and C can be viewed in terms of the "conduction angle," i.e., the percentage of the period for during which the PA is on. As shown in Fig. 28(a), as the conduction angle, θ, decreases, the circuit becomes increas-

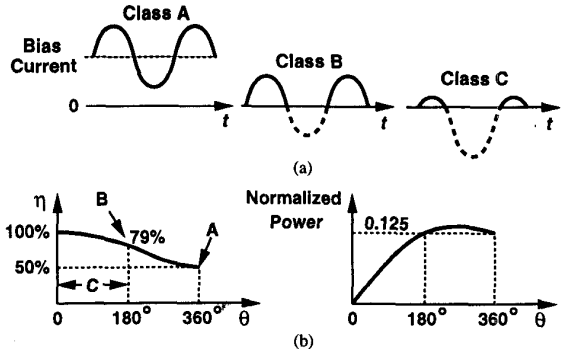

Fig. 28. (a) Signal current waveforms for classes A, B, and C, (b) efficiency and output power vs. conduction angle.

ingly more nonlinear and the output power drops. However, the efficiency, η, rises. In fact, it can be proved that η and the output power vary as illustrated in Fig. 28(b) [8], suggesting that true class C operation is not suited to portable transceivers, where the efficiency at the *maximum* power available from the supply is of greatest interest.

In modern PA design, two other classes, E and F, have emerged as viable choices for high efficiency. Also known as "switching PAs" because their output transistor operates as a switch rather than a current source, class E and F amplifiers are well-suited to constant-envelope modulation systems. The high efficiency is obtained by ensuring that the output transistor sustains a small voltage when it carries substantial current and vice versa, a key property that does not exist in class C stages.

Fig. 29 shows a class E amplifier [9], where the network consisting of C_1, C_2, L_1, and R_L is designed such that the drain

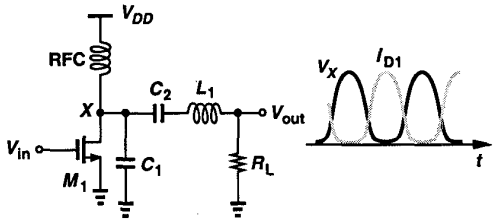

Fig. 29. Class E stage.

current I_{D1} and drain-source voltage V_X of M_1 exhibit negligible overlap in the time domain. Thus, even though the gate and drain voltages of M_1 suffer from a finite transition time, the power consumed by the transistor is small. Class E stages, in theory, achieve an efficiency of 100% while delivering *full* power.

In a class F stage, e.g., Fig. 30, the load network provides a *high* impedance at the second or third harmonic, creating an approximation of a rectangular waveform at the drain of the transistor. Thus, the overlap between the I_D and V_{DS} waveforms can be minimized, leading to efficiencies greater than 85% [10].

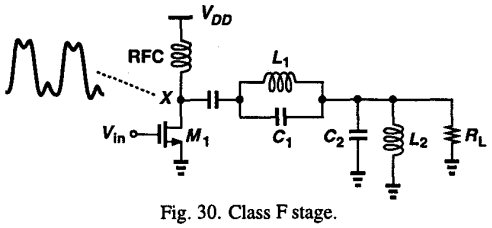

Fig. 30. Class F stage.

V. Design Examples

Fig. 31 depicts a two-stage 900-MHz PA [11]. The driver stage is a class F circuit incorporating two tanks in series, one

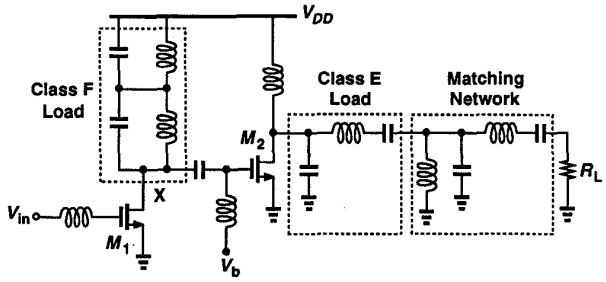

Fig. 31. Two-stage GaAs PA.

tuned to the first harmonic and the other to the third, thereby producing relatively sharp edges at the input of the second stage and switching M_2 rapidly. The output stage is a class E amplifier designed for high efficiency. Fabricated in an 0.8-μm GaAs technology and operating from a 2.5-V supply, the PA delivers an output power of 250 mW with an efficiency of 50%.

A 1.9-GHz CMOS class E PA is shown in Fig. 32 [12]. Configured in fully differential form so as to lower the cur-

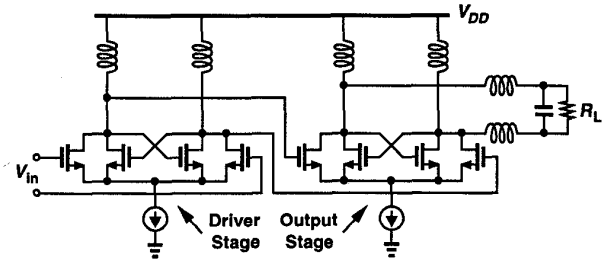

Fig. 32. Two-stage PA using injection-locked oscillators.

rent drawn by each transistor and reduce the substrate noise, the circuit is in fact designed as two cascaded *oscillators*. The idea is that part of the input capacitance of each stage is driven by the stage itself, increasing the overall efficiency. The two oscillators are injection-locked to the input signal - a constant-envelope waveform. Implemented in a 0.35-μm CMOS technology and operating from a 2-V supply, the PA delivers 1 W with 48% efficiency. A point of concern in this design may be injection pulling of the output oscillator by a strong adjacent-channel interferer produced by a nearby user in the transmit band and received by the antenna.

A dual-band CMOS transmitter is shown in Fig. 33 [13]. Designed for operation in the 900-MHz and 1.8-GHz bands, the circuit incorporates two quadrature upconverters driven by a 450-MHz LO so as to generate the quadrature phases of the IF signal with no RC-CR network. The IF signal is subsequently routed to one of two single-sideband mixers driven by a 1350-MHz LO, producing either 900 MHz or 1800 MHz. Fabricated in a 0.6-μm CMOS technology, the transmitter exhibits spurs 40 dB below the carrier while drawing 70 mW from a 3-V supply.

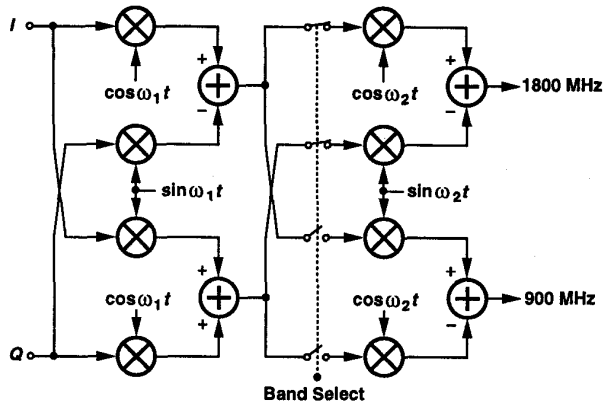

Fig. 33. Simplified architecure of a dual-band transmitter.

References

[1] K. Feher, *Wireless Digital Communications,* Upper Saddle River, New Jersey: Prentice-Hall, 1995.

[2] B. Razavi, *RF Microelectronics*, Upper Saddle River, NJ: Prentice-Hall, 1998.

[3] K. Kurokawa, "Injection Locking of Microwave Solid-State Oscillators," *Proc. IEEE*, vol. 61, pp. 1386-1410, Oct. 1973.

[4] T. D. Stetzler *et al*, "A 2.7-4.5 V Single Chip GSM Transceiver RF Integrated Circuit," *IEEE Journal of Solid-State Circuits,* vol. 30, pp. 1421-1429, Dec. 1995.

[5] T. Yamawaki et al, "A 2.7-V GSM RF Transceiver IC," *IEEE Journal of Solid-State Circuits,* vol. 32, pp. 2089-2096, Dec. 1997.

[6] G. Irvine et al, "An Upconversion Loop Transmitter IC for Digital Mobile Telephones," *ISSCC Dig. of Tech. Papers*, pp. 364-365, Feb. 1998.

[7] L. W. Couch, *Digital and Analog Communication Systems,* Fourth Edition, New York: Macmillan Co., 1993.

[8] H. L. Kraus, C. W. Bostian, F. H. Raab, *Solid State radio Engineering,* New York: Wiley, 1980.

[9] N. O. Sokal and A. D. Sokal,"Class E - A New Class of High-Efficiency Tuned Single-Ended Switching Power Amplifiers," *IEEE Journal of Solid-State Circuits,* vol. 10, pp. 168-176, June 1975.

[10] F. H. Raab, "An Introduction to Class F Power Amplifiers," *RF Design*, pp. 79-84, May 1996.

[11] T. Sowlati et al, "Low Voltage High Efficiency Class E GaAs Power Amplifiers for Wireless Communications," *IEEE Journal of Solid-State Circuits,* vol. 30, pp. 1074-1080, Oct. 1995.

[12] K.-C. Tsai and P. R. Gray, "A 1.9-GHz 1-W CMOS Class E Power Amplifier for Wireless Communications," *Proc. ESSCIRC*, pp. 76-79, Sept. 1998.

[13] B. Razavi, "A 900-MHz/1.8-GHz CMOS Transmitter for Dual-Band Applications," *Symposium on VLSI Circuits Dig. of Tech. Papers*, pp. 128-131, June 1998.